

A LUMINOUS BE+WHITE DWARF SUPERSOFT SOURCE IN THE WING OF THE SMC: MAXI J0158-744

K.L. LI¹, ALBERT K. H. KONG^{1, 6}, P.A. CHARLES², TING-NI LU¹, E.S. BARTLETT², M.J. COE², V. McBRIDE^{3, 4}, A. RAJOELIMANANA^{3, 4}, A. UDALSKI⁵

Draft version July 23, 2012

ABSTRACT

We present X-ray, optical and radio observations of the 2011 transient X-ray source MAXI J0158-744, that reveal some remarkable properties. Detected as a new X-ray transient by MAXI/GSC on 11 November 2011, we followed the subsequent exponential decline of the X-ray light-curve with *Swift* *ToO* observations over the following month. All of the *Swift*/XRT spectra exhibit low temperatures (~ 100 eV) indicating that MAXI J0158-744 is a new Supersoft Source (SSS), and we show how the spectra evolved during the outburst, using blackbody and white dwarf atmosphere models. The *Swift* X-ray spectra near maximum show features around 0.8 keV that we interpret as possible absorption from OVIII and emission from O, Fe and Ne lines. *Swift*/UVOT UV/optical images plus archival OGLE-IV I-band photometry show that the optical counterpart is a bright (13th magnitude) blue star that increased in brightness by approximately 0.5 mag at the time of the MAXI/GSC X-ray flash, and declined on the same timescale as the *Swift*/XRT light-curve. We obtained SAAO and ESO optical spectra of the counterpart early in the outburst and several weeks later. The early spectrum is dominated by strong Balmer and HeI emission, together with weaker HeII emission. The later spectrum reveals absorption features that indicate a B1/2IIIe spectral type, and all spectral features (emission and absorption) are at velocities consistent with the Wing of the SMC. At this distance, it is a luminous SSS ($> 10^{37}$ erg s⁻¹ in the *Swift*/XRT 0.2-2 keV band), but whose brief (< 90 mins) peak luminosity of $> 10^{39}$ erg s⁻¹ in the MAXI/GSC 2-4 keV band makes it the brightest SSS yet seen at “hard” X-ray energies.

We therefore propose that MAXI J0158-744 is a member of the long-sought population of Be-white dwarf binaries, and the first example to possibly enter ULX territory. To account for its properties (very short SSS phase of ≤ 15 d) we deduce that MAXI J0158-744 is a heavy ($\sim 1.35 M_{\odot}$) O-Ne white dwarf which is slowly accreting material from the wind of its early-type companion until it undergoes unstable hydrogen burning on the WD surface, in what is essentially a classical nova explosion. Because the companion to the white dwarf is in this case an early B star, we propose that the brief hard X-ray flash is a result of the shock-heated interaction of the ejected nova shell with the B star wind in which the white dwarf is embedded, and we accordingly draw comparisons with the hard X-rays detected during outbursts of recurrent novae, such as RS Oph, but in a much denser environment. This makes MAXI J0158-744 only the third Be/WD system in the Magellanic Clouds, but it is by far the most luminous. While the SMC has an extensive population of Be X-ray pulsars (and hence are neutron star systems), the detection of their white dwarf cousins is hampered by their greatly reduced optical outburst amplitude and lack of continuous soft X-ray monitoring of these regions. However, the properties of MAXI J0158-744 now gives weight to previous suggestions that SSS in nearby galaxies are associated with early-type stellar systems.

Subject headings: Small Magellanic Cloud, SMC, SSS, Supersoft Source, Magellanic Bridge

1. INTRODUCTION

Supersoft sources (hereafter, SSS) are a class of luminous X-ray sources, so-called because of their very soft ($kT_{\text{bb}} \lesssim 100$ eV) X-ray spectrum, which can reach luminosities up to $\sim 10^{38}$ erg s⁻¹. Initially discovered in the Magellanic Clouds, as a result of their low interstellar absorption in that direction (Long et al. 1981),

they have subsequently been found in the Milky Way and in nearby galaxies (Di Stefano & Kong 2003, 2004a; Kong et al. 2004; Kong & Di Stefano 2005). Key to understanding the nature of the SSS is that their effective black-body radii are comparable to those of a white dwarf. This led to van den Heuvel et al. (1992) establishing what is now considered as the SSS paradigm, wherein they are WDs undergoing super-Eddington accretion in a close binary system which leads to (quasi-)stable thermonuclear burning of hydrogen on the WD surface. Furthermore, this requires a massive WD for the most luminous of the class, and so SSS are considered to be strong candidates as progenitors of Type Ia supernovae in the single degenerate scenario (Di Stefano 2010; Kahabka 2006). SSS are therefore very important for enhancing our understanding of close binary interactions and the late stages of stellar evolution. It also

¹ Institute of Astronomy & Department of Physics, National Tsing Hua University, Taiwan

² School of Physics & Astronomy, University of Southampton, Highfield, Southampton SO17 1BJ, UK

³ University of Cape Town, Private Bag X3, Rondebosch 7701, South Africa

⁴ South African Astronomical Observatory, P.O. Box 9, Observatory 7935, South Africa

⁵ Warsaw University Observatory, Aleje Ujazdowskie 4, 00-478 Warsaw, Poland

⁶ Kenda Foundation Golden Jade Fellow

appears that, under rare circumstances, SSS can exhibit “ultraluminous” (or ULX) levels, which are difficult to explain through a simple application of the steady nuclear burning model.

In late 2011, MAXI J0158-744, a new SSS, was discovered with the MAXI/GSC as a very brief (<90 mins) X-ray flare, in the direction of the Wing of the Small Magellanic Cloud (SMC), but with poor (~ 0.5 degree) location accuracy (Kimura et al. 2011). This X-ray flare (denoted XRF 111111A) exhibited a very unusual X-ray spectrum in that all the X-ray flux was confined to the lowest GSC energy channel (2–4 keV), inferring a luminosity at these energies of $> 6 \times 10^{38}$ (Kimura et al. 2011) at the distance of the SMC. This was substantially higher than any known Galactic/Magellanic Cloud SSS, and approaching the luminosities seen in some extragalactic SSS (Greiner 2000).

A *Swift* X-ray and UV/optical observation (Kennea et al. 2011; Li & Kong 2011b) was performed within 10 hours of the MAXI trigger, revealing that MAXI J0158-744 was a new, luminous SSS ($2 \times 10^{37} \text{ erg s}^{-1}$ (0.2–2 keV), and with an accurate (± 2.3 arcsecs) location of R.A.=01:59:25.55, Dec.=−74:15:28.6, J2000.0). The X-ray spectra were compatible with a low temperature blackbody ($kT_{\text{bb}} \sim 100$ eV) that is typical of the SSS.

Ultraluminous X-ray sources (ULXs) are non-nuclear X-ray sources with $L_X \geq 10^{39} \text{ erg s}^{-1}$, whose physical properties are still controversial (Swartz et al. 2004). Short-term variability indicates that they must be accreting compact objects, where the mass transfer rate is close to or exceeding the Eddington Limit. Once strong candidates for the long-sought intermediate-mass black holes, they are now considered likely to be extreme examples of stellar-mass black holes (see e.g. Zampieri & Roberts (2009)). It is thus of considerable current interest as to how accreting WDs can even come close to having properties that appear to overlap with the ULX.

In this paper, we present a time-resolved, multi-wavelength follow-up of the MAXI J0158-744 X-ray flare and its subsequent decline over the next few months, using *Swift* XRT/UVOT, GALEX, SAAO 1.9m, ESO NTT, WISE and ATCA radio observations to reveal some of the detailed properties of this remarkable object. It is almost certainly a WD, and its normal stellar companion is an early-type Be star, making MAXI J0158-744 the prime example of the long-sought Be/WD binary population in the Magellanic Clouds.

2. OBSERVATIONS

2.1. X-ray: MAXI

The MAXI X-ray camera monitors the 0.5–30 keV X-ray sky from the International Space Station, providing source alerts and making its data immediately publicly available⁷. MAXI J0158-744 was detected by the MAXI/GSC on November 11, 2011 as a bright, but short-lived (less than a single 92 min orbit) soft X-ray flare (for details see Kimura et al. (2011)). Using the on-line processed data products provided by the MAXI team (i.e. light curve and spectrum) we show in figure 1 (top panel) the MAXI/GSC light curve (at the highest tem-

poral resolution of orbit by orbit) in the lowest energy band provided (2–4 keV). Remarkably, apart from the clear X-ray flare that was detected from 2011-11-11 03:34 to 05:06 UTC with a count rate of $0.42 \pm 0.05 \text{ cts s}^{-1}$ (400 mCrab), the source is virtually undetectable at all other times in this 4 month interval.

The MAXI X-ray spectrum corresponding to the X-ray flare indicates only that it was soft (confined to the lowest energy channel) and so we fitted it with an absorbed blackbody model, and with the column density (N_{H}) fixed to the galactic value of $4.0 \times 10^{20} \text{ cm}^{-2}$ (Dickey & Lockman 1990) and the temperature to 400 eV (as quoted in Kimura et al. (2011)). Given its location (in the direction of the SMC, and confirmed by our optical spectra below) we assume a distance of 61.3 kpc (Hilditch et al. 2005; Kimura et al. 2011), which leads to an unabsorbed luminosity in the flare of $\sim 2 \times 10^{39} \text{ erg s}^{-1}$ (2–4 keV). This immediately established great interest in MAXI J0158-744 as potentially the most luminous SSS in the Magellanic Clouds ever reported (see Greiner (2000) for a compilation of known SSS). Furthermore, this extremely high luminosity places MAXI J0158-744 into the ULX regime, bearing comparison with sources usually interpreted as high mass transfer black-hole systems (see Hodges-Kluck et al. (2012); Soria et al. (2012)).

For comparison with the black-body model, we also fitted a Raymond-Smith thermal plasma model. This gave a similar unabsorbed luminosity, and with a best fit temperature of ~ 0.9 keV. The signal to noise of the MAXI spectrum does not allow a distinction between the models.

2.2. X-ray: Swift/XRT

TABLE 1
Swift OBSERVATIONS OF MAXI J0158-744

Obs Id	Date ^a (m/d)	Exp(XRT) (s)	Exp(UVOT) (s)	Mode ^b (PC/WT)
32181001	Nov 11	682	867	PC
32182001	Nov 11	735	912	PC
32187001	Nov 12	1994	1950	WT
32187002	Nov 14	1994	1956	WT
32187004	Nov 15	2024	1966	WT
32187005	Nov 16	2169	2111	WT
32187006	Nov 17	1724	1676	WT
32187007	Nov 18	2146	2097	PC
32190001	Nov 19	4351	4316	PC
32190002	Nov 19	707	667	PC
32187008	Nov 20	2567	2517	PC
32187010	Nov 22	2292	1570	PC
32187011	Nov 23	2337	2286	PC
32187012	Nov 24	2339	2262	PC
32187013	Nov 25	1354	1316	PC
32187014	Nov 26	2448	2398	PC
32187015	Dec 9	1983	1925	PC
32187016	Dec 23	3677	2481	PC

^aAll observations were taken in 2011.

^bPC: Photon-Counting; WT: Window-Timing.

MAXI J0158-744 was observed by *Swift* between November and December 2011 (see Table 1). The first two observations were taken in photon counting (PC) mode in order to accurately locate the source, since the MAXI all-sky camera only provides ~ 0.4 degree po-

⁷ <http://maxi.riken.jp/mxondem/>

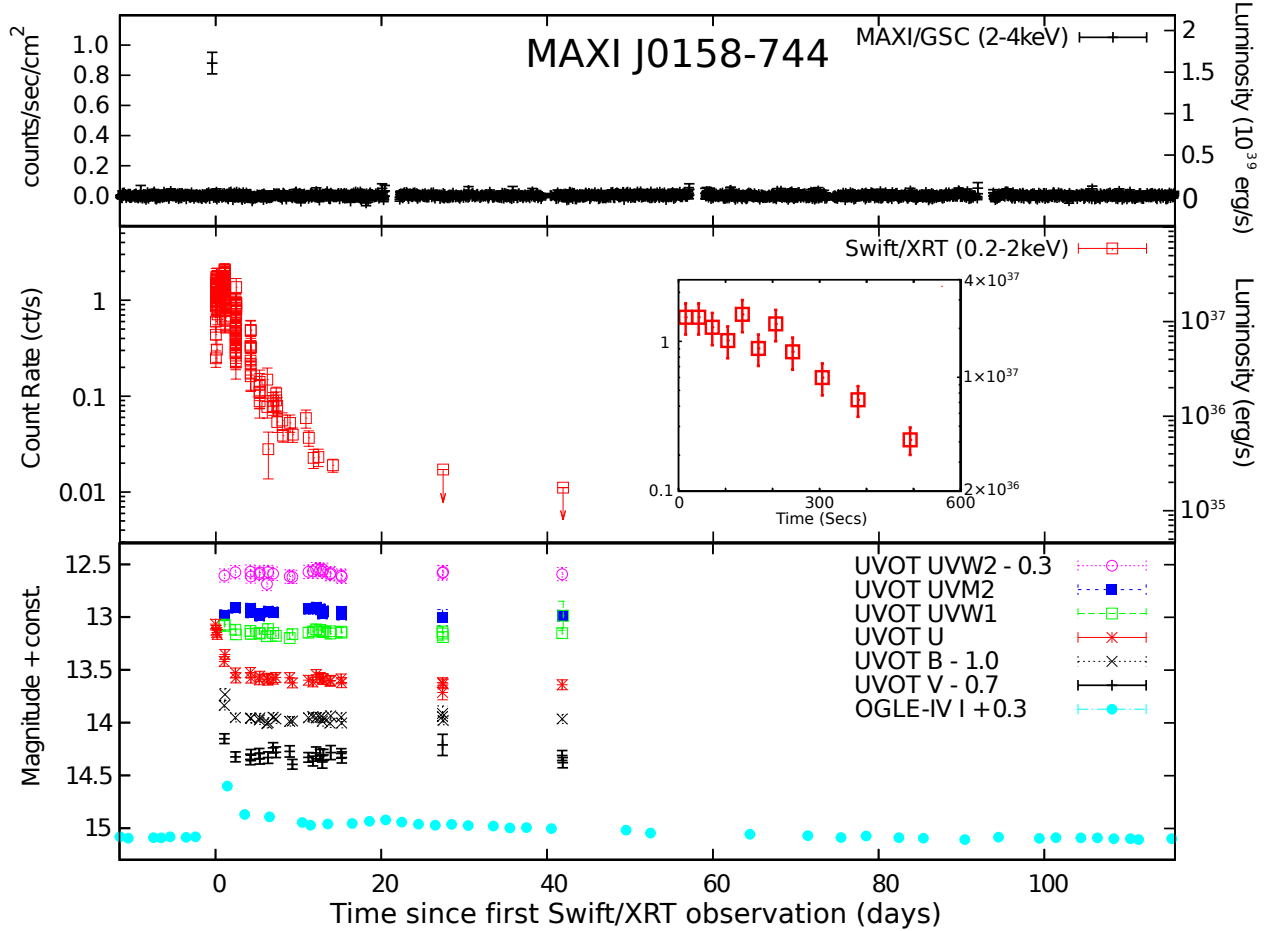


FIG. 1.— Multi-wavelength lightcurves of MAXI J0158-744 from hard X-ray to optical, covering the interval from 2011 Oct 31 to 2012 Mar 06, and with the time axis referenced to that of the first *Swift* observation (2011 Nov 11 15:33 UT). Upper panel: MAXI/GSC 2–4 keV lightcurve with time resolution of 92 mins (single orbit). The X-ray flash is clearly visible close to time zero, and the X-ray luminosity (right-hand axis) is given for the unabsorbed black-body model and SMC distance (see text for details); middle panel: *Swift*/XRT X-ray lightcurve (0.2–2 keV). The X-ray luminosity (right-hand axis) is given for the X-ray spectral fit corresponding to the peak of the lightcurve and is intended as a guide only (see text). The inset box shows how the X-ray flux declined by almost an order of magnitude during the first 500 seconds observation; lower panel: *Swift*/UVOT lightcurves covering 6 bands from the near-UV to optical, plus the OGLE-IV I-band lightcurve.

sitional information (Kimura et al. 2011)). Subsequent observations were taken in window timing (WT) mode, in order to reduce pile-up effects due to the high initial count-rate ($> 0.6 \text{ count s}^{-1}$), and then returned to PC mode for the last 11 observations. Data calibration, extraction and event filtering were performed according to standard procedures outlined in the *Swift*/XRT data reduction guide (Capalbi et al. 2005).

Unlike most Galactic soft X-ray transients (e.g. XTE J1200+521 (Smith & Remillard 2003)), the outburst of this source lasted barely two weeks, and within a month it was below the *Swift* detection limit, indicating a two orders of magnitude drop in intensity (Fig 1). In order to search for any rapid periodicities, we performed a Fourier analysis of the MAXI and *Swift* data. However, no significant signal was present in the power spectra.

We then established different time intervals for analysis based on the flux levels in the overall light-curve, producing summed spectra for each time period of interest. As the first two observations in Table 1 are essentially a single observation, we merged them to form a combined spectrum. In the following three observations (Nov 12–15), the X-ray source was still strong, and

therefore we grouped them individually. We combined the remaining observations as follows in order to increase the signal-to-noise ratio: Nov 16–17; Nov 18–20, 22–26. The final two observations were not used, as the source, while marginally detected, was too weak to produce useable spectra.

2.2.1. XRT Spectral Fitting

The X-ray spectra were fitted with *XSPEC* (Arnaud 1996) using mostly blackbody models, but we also tried the Tübingen white dwarf model atmospheres (Rauch & Deetjen 2003; Werner & Dreizler 1999; Werner et al. 2003) which can be used in *XSPEC* as a tabular grid of models for fitting. Nevertheless, all the temperatures relevant here are low ($\sim 100 \text{ eV}$), which makes the results (especially the implied luminosity) extremely sensitive to the N_{H} values of the fit. Accordingly, we assumed the presence of a Galactic N_{H} value of $4 \times 10^{20} \text{ cm}^{-2}$ (Dickey & Lockman 1990) in all models, so as to avoid overestimating the unabsorbed flux or underestimating the temperature. All the XRT spectra give temperatures in the range 80–120 eV (see top half of Table 2). The inferred luminosities decrease exponen-

tially from the initial peak, and the source drops below the *Swift* detection limit about a month later (Fig. 1). However, it should be noted that the source and its spectrum varied dramatically from early in the outburst (as demonstrated by the hardness ratio and X-ray flux plots (Fig 3 and the inset in Fig 1). Hence a blackbody may not be appropriate to account for all phases of the outburst. Nonetheless, the fit parameters are still useful for comparison with other soft X-ray transients.

In addition to the fixed N_H blackbody fitting, we tried adding an additional absorbing component to see if there is any intrinsic absorption in the system. This extra absorption had abundances set to those appropriate for the SMC (Russell & Dopita 1992). Except for the last spectrum (that required no additional absorption), the fits to all other spectra were significantly improved. However, many of the parameters are not then well constrained, especially the normalization factors (which are important for estimating the blackbody radius), and so these are given as upper limits in the lower half of Table 2.

We also attempted to find a better model by trying various model combinations. We found that an absorption edge at 0.9 keV and an emission line at 0.7 keV⁸ can ameliorate the fits of November 11 and 12, respectively. The best fit parameters for these models are shown in parentheses in Table 2, and all the models plotted in Fig 2.

In addition to the detailed spectral analysis, we investigated both short and long timescale spectral variability in MAXI J0158-744 by plotting the spectral hardness ratio (HR, defined as $HR = (M - S)/(M + S)$) against the X-ray lightcurve. The soft (S) and medium bands (M) cover 0.2–0.5 keV and 0.5–2.0 keV, respectively. We find (Fig 3) that HR varied throughout most of the observations, especially in the early and late times of the outburst, when the changes are correlated with the X-ray flux (i.e. a lower count rate gives a harder spectrum). Furthermore, we noted a jump in HR on 2011-11-12 at 17:16 UTC from 0.13 ± 0.05 to 0.41 ± 0.10 which is clearly visible in the middle panel of Fig 3. We divided the spectra accordingly and found that the jump was associated with the sudden appearance of the 0.7 keV emission feature required by the fits (Fig 2).

2.3. UV/optical: *Swift*/UVOT

Simultaneously with the *Swift*/XRT observations, UVOT images in six UV to optical filters were obtained, with ~ 100 s per exposure (except for the very first observation, that was U-band only). We performed aperture photometry on these data, using standard UVOT procedures (Romig et al. 2005) to obtain lightcurves. To optimize the signal-to-noise ratio, we used an aperture radius of $3''$ as recommended by HEASARC (Burrows et al. 2005) and a source-free background region that minimizes contamination from nearby sources.

We also obtained a single 5000 s UVOT optical spectrum (2800–5200 Å) on 2011 Nov 19. This was processed using standard UVOT procedures and background subtracted. Wavelength calibration is limited by the extended shape of the zeroth order image to an accu-

racy ~ 10 Å, and a systematic offset of up to 66 Å (see Bufano et al. (2009) for details). There are no obvious emission/absorption features present, but it is brighter at shorter wavelengths, as indicated by the photometry.

2.3.1. UVOT Results

In the early part of the MAXI J0158-744 outburst, our UVW1, U, B and V images show significant brightening, by up to ~ 0.5 mag, followed by a rapid decline (within days) to a stable level (Fig. 1). In contrast, the UVM2 and UVW2 levels stayed almost constant, at $UM2 \sim 13.0$ and $UW2 \sim 12.9$ (with uncertainty ~ 0.05 mag during the entire *Swift* campaign. Assuming the Galactic column of $N_H = 4.0 \times 10^{20} \text{ cm}^{-2}$, we estimated the V-band extinction as $A_V = 0.03$ (Gordon et al. 2003). We then used the SMC Bar's extinction curve (Gordon et al. 2003) to estimate the extinction values for the other bands: $A_B = 0.04$, $A_U = 0.05$, $A_{UW1} = 0.07$, $A_{UM2} = 0.09$, and $A_{UW2} = 0.11$. (Some data were excluded from this analysis as a result of spacecraft pointing drifts, which clearly produced spurious results.)

2.4. Optical: OGLE-IV monitoring

MAXI J0158-744 is located in a region of the SMC that is monitored by the OGLE-IV project (Udalski 2008). Consequently, this provides us with close to nightly monitoring of the source, both before and during the interval covered by the *Swift* observations. As expected, there is a bright optical source present in the OGLE images, at R.A.=01:59:25.87, Dec.=−74:15:28.0 (J2000.0), which is well within the *Swift*/XRT error circle. The OGLE data are restricted to the I-band, and are plotted as the bottom curve of Fig. 1. A major optical flare (reaching $I=14.3$) is clearly seen at the time of the X-ray flash. In fact, this point was obtained 1–2d after the X-ray flash, which means that the peak I-band magnitude could be even higher.

From the OGLE monitoring prior to the data plotted here, we find that $I=14.82 \pm 0.01$ from 500d to 320d before the X-ray flash. At this point, the optical light increased to a new quasi-quietest magnitude (14.79 ± 0.01), which persisted up to the major flare.

Besides the major flare, we also note a secondary peak almost exactly 20d after the main outburst. Curiously there is a small-scale “blip” in the MAXI/GSC lightcurve at the same time (Fig. 1). However, the signal-to-noise ratio of the MAXI/GSC data here is so weak ($S/N=1.7$), that we cannot claim this is a real signal. Unfortunately, no *Swift* XRT/UVOT observations were carried out during that period.

2.5. Optical spectroscopy: SAAO/1.9m

A low resolution, wide wavelength ($\lambda\lambda 4000$ –7700) optical spectrum of MAXI J0158-744 was obtained with the SAAO 1.9m telescope and CCD spectrograph at Sutherland, South Africa on 2011 Nov 16, beginning at 22:23UT, approximately 5 days after the initial X-ray flash. Two 1800s exposures using the SITe CCD camera and 300 l/mm grating (giving 7Å resolution) were obtained within a timespan of 2 hours, and the average of these is plotted in figure 4. It is dominated by very strong Balmer emission, but also exhibits strong HeI emission at $\lambda 5876$ and $\lambda 6678$, and weaker HeII $\lambda 4686$

⁸ It has been suggested that the 0.7 keV excess could be explained by an over-abundance of oxygen and neon along the line of sight (Juett et al. 2001).

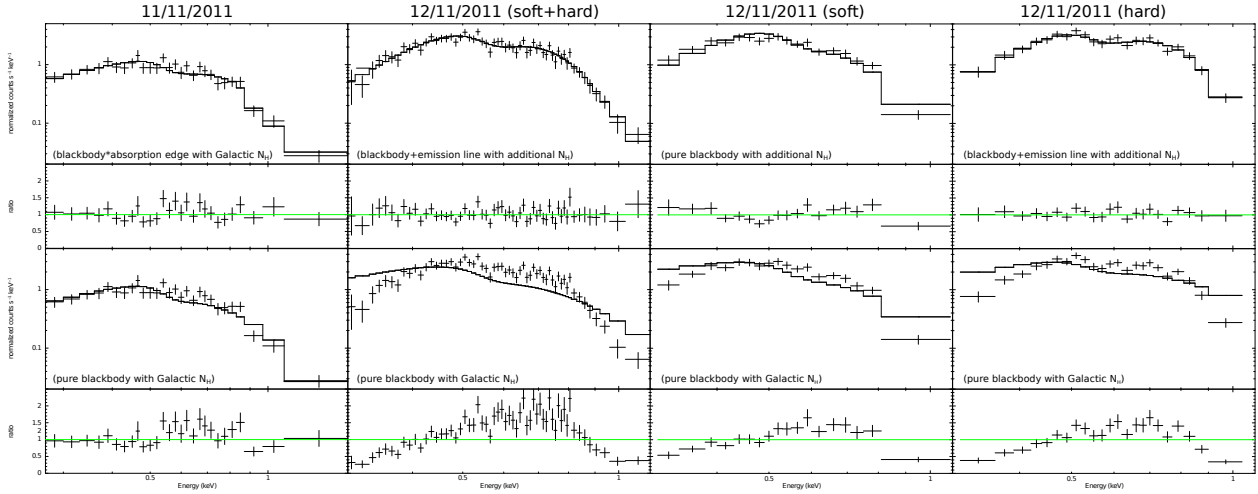


FIG. 2.— Early outburst *Swift*/XRT spectra of MAXI J0158-744 with their best fit models (below which are plotted the residuals to the fits): left column: (upper) 11 Nov spectrum with blackbody + absorption edge at 0.89keV (and fixed Galactic N_H), and (lower) pure blackbody with fixed Galactic N_H of $4 \times 10^{20} \text{ cm}^{-2}$; 2nd column: (upper) 12 Nov spectrum with blackbody plus an emission line with additional N_H and (lower) pure blackbody with fixed Galactic N_H of $4 \times 10^{20} \text{ cm}^{-2}$. Right two columns show the spectra and fits when dividing the 12 Nov spectrum to be before (soft) and after (hard) the HR jump seen in Fig 3. The “hard” (right) spectrum includes a broad emission feature at 0.7keV. Note that the absorption and emission features are visible in the residuals to the simple fits.

emission. Such emission clearly identifies this object with the X-ray outburst, and has characteristics of both BeX and SSS sources. However, the spectrum does contrast that of the prototype SSS, CAL83, where HeII $\lambda 4686$ is by far the dominant emission feature in the spectrum (Crampton et al. 1987).

2.6. Optical spectroscopy: ESO/FOS

Optical spectra were taken on 2011 Dec 8 (almost 1 month after the initial X-ray flash) with the ESO Faint Object Spectrograph (EFOSC2) mounted at the Nasmyth B focus of the 3.6m NTT. A slit width of $1.5''$ was employed, together with a $600 \text{ lines mm}^{-1}$ grating that yielded 1 \AA pixel^{-1} dispersion over a wavelength range of $\lambda\lambda 3095\text{--}5085 \text{ \AA}$. The resulting spectra were recorded on a Loral/Lesser, thinned, AR-coated, UV flooded, MPP CCD with 2048×2048 pixels, at a spectral resolution of $\sim 10 \text{ \AA}$. The data were reduced using the standard packages available in the Image Reduction and Analysis Facility (IRAF). Wavelength calibration was achieved with Helium and Argon arc lamps, and the data were reduced using IRAF. The resulting spectrum of MAXI J0158-744 was normalized to remove the continuum and then redshift-corrected for an assumed SMC recession velocity of -158 km s^{-1} .

2.6.1. Spectral Classification

OB stars in the Milky Way are classified using certain metal and helium line ratios (Walborn & Fitzpatrick 1990), but this cannot be applied in lower metallicity environments, such as the SMC, due to the weakness or absence of the metal lines. Accordingly, we classified the spectrum of MAXI J0158-744 using the method of Lennon (1997) for B-type stars in the SMC.

Figure 5 shows the unsmoothed optical spectrum of MAXI J0158-744, which is dominated by the Balmer and neutral helium lines. The HeII $\lambda\lambda 4200, 4143$ lines are either too weak or absent, which makes the optical counterpart later than O9. The SiIII $\lambda 4553$ line is stronger

than MgII $\lambda 4481$, implying a spectral classification earlier than B2.5. There does appear to be some evidence for the SiIV $\lambda 4116$ line, however the rotationally broadened H δ line in close proximity makes it difficult to distinguish. As such we classify the optical counterpart of MAXI J0158-744 as a B1-2 star.

As to its luminosity class, a B1-2 main sequence star would have M_V of -3.2 to -2.5 . However, the lowest V measurement in fig 1 is 14.2 (corrected for the Galactic extinction), which corresponds to $M_V = 4.7$ (for $d = 61.3 \text{ kpc}$), which is closer to the brightness of a giant. This is also typical of many other BeX systems in the SMC (Bird et al. 2012).

2.7. ATCA Observations

MAXI J0158-744 was observed by ATCA on December 23, 2011. The observations were performed simultaneously at frequencies 5.5 GHz and 9 GHz with configuration 6A (with the baseline ranging from 337 m to 6 km) and the upgraded Compact Array Broadband Backend (CABB). The data was taken with the CFB 1M-0.5k correlator configuration with 2 GHz bandwidth and 2048 channels, each with 1 MHz resolution. The primary calibrator used was 1934-638, while the phase calibrator was 0230-790. At the start of each observation, we observed 1934-638 for 10 min. The phase calibrator was observed every 25 min. We used MIRIAD (Sault et al. 1995) to analyse the data with standard procedures. We then perform standard data reduction steps, including band-pass, phase and amplitude calibrations. When producing the dirty maps. We used the multi-frequency synthesis (MFS) method (Sault & Conway 1999) and natural weighting to suppress the noise. The effective on-source integration time of MAXI J0158-744 is 3.8 and 3.4 hours for frequencies 5.5 GHz and 9 GHz, respectively. The field of view of ATCA with configuration 6A is $\sim 10'$ and $5'$ for 5.5 GHz and 9 GHz, respectively, and with spatial resolution that can reach $\sim 1''$ to $2''$.

2.7.1. ATCA Results

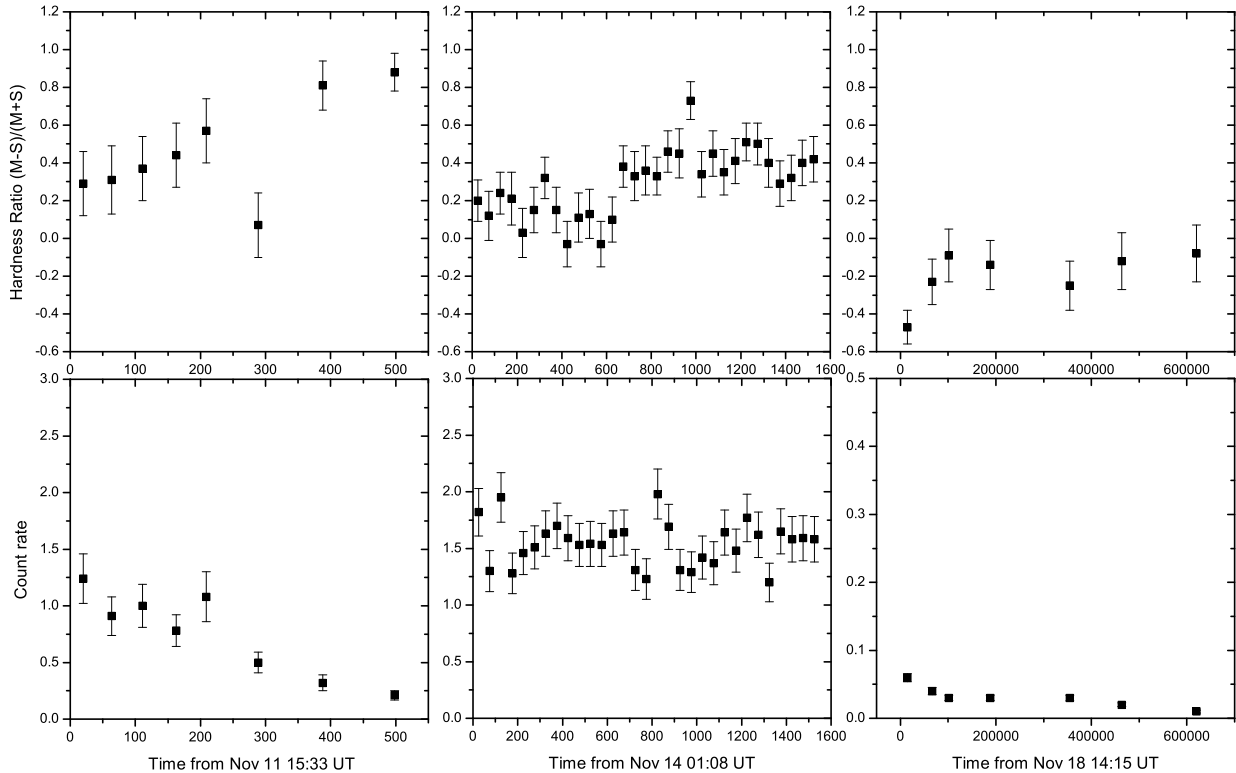


FIG. 3.— Demonstration of the X-ray spectral variability exhibited by MAXI J0158-744. Upper panels: plot of hardness ratio, defined as $(M-S)/(M+S)$, against time; lower panels: corresponding X-ray lightcurve. The first and the third boxes show a tentative correlation between the X-ray intensity and hardness ratio on quite different time-scales, while the middle box shows a clear hardness ratio jump, which occurs when the 0.7 keV emission feature turns on (see text).

Fig. 6 shows the *Swift* X-ray images overlaid with ATCA radio map contours of MAXI J0158-744. Besides background quasars, we did not detect any significant ($>3\sigma$) radio sources at the MAXI J0158-744 location. However, there is a very marginal signal ($\sim 2\sigma$) detected within the XRT error circle, which will require deeper exposures to confirm. In naturally weighted maps, the rms noise level for MAXI J0158-744 is 16 (5.5 GHz) and 25 (9 GHz) $\mu\text{Jy}/\text{beam}$. We combined the observations from different frequencies in order to reduce the rms noise level at 6.8 GHz, but the improvement is not significant due to the short integration time. As a result, the observations reached a rms noise level of 15 $\mu\text{Jy}/\text{beam}$, giving a 3σ upper limit of $\sim 45 \mu\text{Jy}/\text{beam}$ for MAXI J0158-744. Although we did not find any statistically significant radio emission at the X-ray position, there is a 9.3σ detection ($\sim 150 \mu\text{Jy}/\text{beam}$) at 5.5 GHz approximately $25''$ away, while this source was not detected at 9 GHz. We further calculated a lower limit of 0.54 to its spectral index (α) by using the flux density at 5.5 GHz and the rms at 9 GHz. This is consistent with a background AGN (Nandra et al. 2005; Tozzi et al. 2006).

2.8. Archival measurements

There is an optical/IR source listed in the SuperCOSMOS (Hambly et al. 2001b) and 2MASS (Skrutskie et al. 2006) catalogs that has been associated with MAXI J0158-744 (Kennea et al. 2011; Li & Kong 2011b). Quoted magnitudes are $B_J=15.05$, $R_2=14.898^9$,

⁹ For R-band photometry, we used R_2 in preference to R_1 since the former has higher signal-to-noise and better calibration.

$I=14.885$, $J=14.8$, $H=14.8$, and $K=14.4$. The B-band value is consistent with our UVOT low-state measurements. The 2MASS values are consistent with measurements from a quite separate IR study of the Magellanic Bridge, where the quoted values are $J=14.78 \pm 0.01$, $H=14.65 \pm 0.02$, and $K_s=14.38 \pm 0.02$ (Nishiyama et al. 2007). Furthermore, we also found counterparts of MAXI J0158-744 in the Galaxy Evolution Explorer (GALEX) catalog (GR6: 14.66 ± 0.02 and NUV: 14.64 ± 0.01) and the Wide-field Infrared Survey Explorer (WISE) catalog ($w1=14.02 \pm 0.03$, $w2=13.74 \pm 0.03$, $w3=12.54 \pm 0.29$, and $w4 > 9.78$).

2.8.1. Spectral Energy Distribution

Using all the quiescent photometric measurements plus the two ATCA upper limits, we produced a SED from 5.5 GHz (5.45 cm) to 155 PHz (1928 \AA) (Fig. 7). After applying extinction corrections (Gordon et al. 2003), the SED can be represented as a power law of index 1.7. However, we caution that the extinction corrections may not be fully applicable in this region (we used the SMC Bar extinction curves), and hence the SED shape is only approximate.

3. DISCUSSION

3.1. Nature of the compact object and mass donor in MAXI J0158-744

The sequence of *Swift*/XRT spectra obtained throughout the outburst of MAXI J0158-744 have properties that are typical of classical SSS in the Magellanic Clouds, principally low temperature ($\sim 100\text{eV}$) thermal X-ray

TABLE 2
Swift/XRT SPECTRAL PROPERTIES OF MAXI J0158-744

Date	N _H (Additional) 10 ²⁰ cm ⁻²	Unabsorbed $L_X(0.2-2\text{keV})$ 10 ³⁷ erg s ⁻¹	Blackbody Temperature eV	Radius 10 ⁴ km	χ^2/dof	Notes
Blackbody + fixed N _H of $4 \times 10^{20} \text{ cm}^{-2}$ (wabs*bbbodyrad)						
11/11/2011	...	$2.1^{+0.1}_{-0.1}$	108^{+4}_{-3}	$0.12^{+0.01}_{-0.01}$	40/26	...
12/11/2011	...	$2.4^{+0.1}_{-0.1}$	114^{+3}_{-2}	$0.11^{+0.01}_{-0.01}$	457/56	...
14/11/2011	...	$0.99^{+0.05}_{-0.09}$	81^{+4}_{-4}	$0.16^{+0.03}_{-0.02}$	40/18	...
15/11/2011	...	$0.49^{+0.04}_{-1.3}$	83^{+11}_{-10}	$0.11^{+0.05}_{-0.03}$	12/7	...
16–17/11/2011	...	$0.28^{+0.01}_{-0.02}$	95^{+6}_{-6}	$0.06^{+0.01}_{-0.01}$	39/10	...
18–26/11/2011	...	$0.09^{+0.01}_{-0.01}$	92^{+5}_{-6}	$0.04^{+0.01}_{-0.01}$	44/14	...
Blackbody + additional N _H (phabs*vphabs*bbbodyrad) ^c						
11/11/2011 ^d	$14^{+16}_{-12} (< 13)$	$28.2^{+0.1}_{-0.4} (< 1.9)$	$102^{+7}_{-7} (122^{+8}_{-11})$	$0.16^{+0.06}_{-0.04} (0.09^{+0.04}_{-0.01})$	38.0/25 (22.9/23)	(+ edge at $0.89 \pm 0.03 \text{ keV}$)
12/11/2011 ^e	$177^{+31}_{-27} (139^{+39}_{-43})$	$\lesssim 146 (< 67)$	$63^{+4}_{-4} (65^{+6}_{-7})$	$3.5^{+2.6}_{-1.4} (< 2.2)$	60.1/55 (47.5/52)	(+ line at $0.7^{+0.1}_{-0.2} \text{ keV}$)
14/11/2011	86^{+47}_{-36}	$\lesssim 14.8$	56^{+8}_{-9}	$\lesssim 1.6$	12.5/17	...
15/11/2011	67^{+109}_{-59}	$\lesssim 4.5$	58^{+23}_{-23}	$\lesssim 0.8$	8.2/6	...
16–17/11/2011	< 234	$\lesssim 2.6$	52^{+24}_{-24}	$\lesssim 0.8$	10.5/8	...
18–26/11/2011 ^f
WD atmosphere model + fixed N _H (wabs*tmmap) ^g						
11/11/2011	...	$\lesssim 1.6$	90.5 (max)	...	212/26	...
12/11/2011	...	$\lesssim 1.9$	90.5 (max)	...	1408/56	...
12/11/2011 (soft)	...	$\lesssim 2.2$	90.5 (max)	...	537/34	...
12/11/2011 (hard)	...	$\lesssim 1.8$	90.5 (max)	...	557/44	...
14/11/2011	...	$0.72^{+0.07}_{-0.02}$	90.5 (max)	...	21/18	...
15/11/2011	...	$\lesssim 0.36$	90.5 (max)	...	36/7	...
16–17/11/2011	...	$\lesssim 0.21$	90.5 (max)	...	94/10	...
18–26/11/2011	...	$0.07^{+0.01}_{-0.01}$	90.5 (max)	...	127/14	...
WD atmosphere model + additional N _H (phabs*vphabs*tmmap) ^g						
11/11/2011	15^{+2}_{-2}	$\lesssim 8.4$	90.5 (max)	...	174/25	...
12/11/2011	$24^{+2}_{-1} (12^{+3}_{-2})$	$\lesssim 17 (< 6.2)$	90.5 (max)	...	151/55 (61/53)	E _{gau} = 0.7 (fixed)
12/11/2011 (soft)	84^{+14}_{-13}	$\lesssim 11$	90.5 (max)	...	59/33	...
12/11/2011 (hard)	$32^{+3}_{-2} (30^{+2}_{-3})$	$\lesssim 29 (24^{+231}_{-7})$	90.5 (max)	...	131/43 (90/41)	E _{gau} = 0.7 (fixed)
14/11/2011	$\lesssim 5.1$	$0.91^{+0.05}_{-0.07}$	90.5 (max)	...	19/17	...
15/11/2011 ^f
16–17/11/2011 ^f
18–26/11/2011 ^f

^aUpper limits are shown for those parameters with lower limits pegged to zero OR where irrational errors were obtained (i.e. best-fit value lies outside the error range) during 1- σ error calculations.

^bFor those fits with $\chi^2_{\nu} > 2$, we used *cstat* to re-fit and calculate the errors.

^cN_H of $4 \times 10^{20} \text{ cm}^{-2}$ with solar abundances was included as a fixed contribution to the absorption within the Galaxy.

^dAn absorption edge was included in the model where the best-fit threshold energy is shown in the **Notes** column and the resulting parameters are shown in parentheses.

^eAn additional Gaussian emission line is included in the model where the best-fit emission energy is shown in the **Notes** column and the resulting parameters are shown in parentheses.

^fNo valid fit was found.

^gAll best fit temperatures reach the maximum value (1.05 million K) allowed for the WD atmosphere model.

emission (after the initial flash) that is likely the consequence of thermonuclear burning of hydrogen on the surface of a white dwarf. Furthermore, the optical spectra have features whose velocities are consistent with the system being located in the Magellanic Bridge; and the spectral absorption features later in the decline identify the mass donor as an early-type star, likely B1-2IIIe. Combined with the inferred blackbody radius of the SSS (about 0.001–0.01 R_⊙), we therefore conclude that MAXI J0158-744 is a white dwarf (WD) orbiting a Be star.

There is now a consensus on the accretion rate regimes and masses in which persistent and transient SSS occur, and this has recently been reviewed by Kato (2010). This can be summarised briefly as follows:

- $10^{-7} - 4 \times 10^{-7} M_{\odot} \text{ yr}^{-1}$, in this relatively narrow range of mass transfer rates, accreting white dwarfs (of mass 0.7–1.2 M_{\odot}) burn hydrogen on their surfaces steadily without driving substantial outflows, and are seen as persistent SSS;

- *below* $10^{-7} M_{\odot} \text{ yr}^{-1}$, the hydrogen burning is triggered sporadically, which is normally seen as a nova explosion (either classical or recurrent). During the later phases of the nova outburst, the system will enter an SSS phase, the duration of which is a strong function of the white dwarf mass, with the highest masses producing the shortest durations (Kato 2010) and references therein;
- *above* $4 \times 10^{-7} M_{\odot} \text{ yr}^{-1}$, the hydrogen burning drives substantial outflows which is seen as an optically thick wind. However, this wind can interact with the low mass donor in ways that can temporarily stop the Roche lobe overflow, which will then cause the SSS to switch off. Subsequently, the mass transfer onto the white dwarf restarts and the process is repeated. The prototype of this behaviour is RXJ0513.9-6951 (Southwell et al. 1996).

Based on this interpretation, MAXI J0158-744 fits the

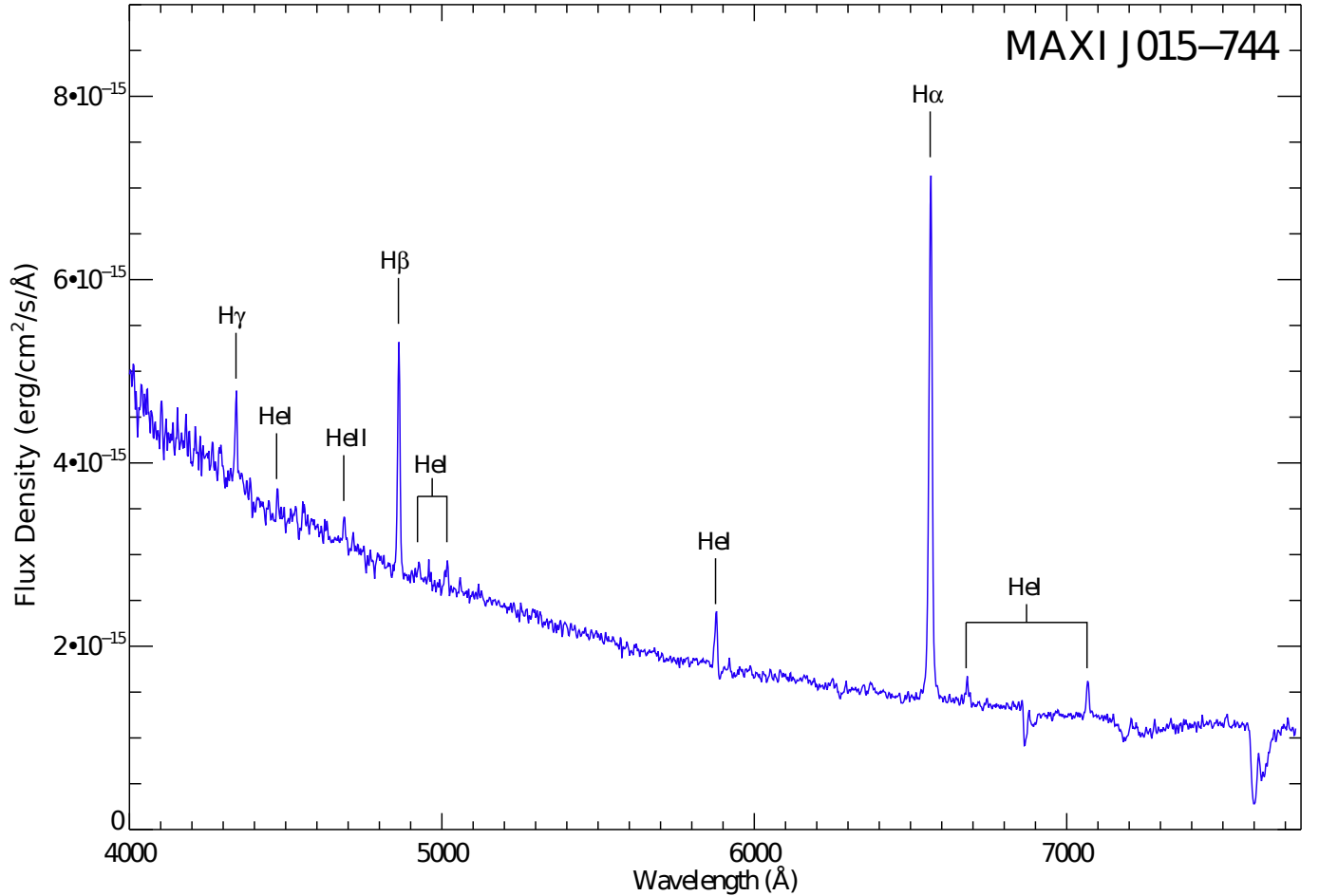


FIG. 4.— Low resolution optical spectrum of MAXI J0158-744 obtained with the SAAO/1.9m on 2011-11-16. The spectrum has been flux calibrated and redshift corrected by -158 km s^{-1} . Dominant emission features are marked.

second (low mass transfer rate) explanation extremely well, and so we can constrain the mass accretion rate onto the white dwarf in MAXI J0158-744 to be less than a few times $10^{-7} M_{\odot} \text{ yr}^{-1}$. But what about the nova explosion that should have been associated with this event? In fact, typical novae in the SMC have peak magnitudes in the range 11–13.6 (Greiner 2000), but these are all classical or recurrent novae, where the mass donor is a low mass star (and hence intrinsically faint). In the case of MAXI J0158-744, the donor is intrinsically a luminous star in its own right, and so the approximately 0.5–1 mag increase observed here (Fig 1) is entirely consistent with a classical or recurrent nova event taking place in the company of an early-type star.

That there are multiple emitting components in this system is clear from the different temporal behaviour that is a strong function of wavelength. The X-ray/optical lightcurves (Fig. 1) do show a clear positive correlation, where the X-ray emission drops exponentially for about two weeks and the U-band light drops even faster (at a rate of 0.5 mag in 2.4 d). More significantly, the duration of the optical outburst is about 6 times shorter than that of the X-ray outburst. MAXI J0158-744 also shows significant excess (0.1–0.5 mag) in the other three longer wavelength (B, V, UW1), yet no significant excess can be found at shorter wavelengths (UM2, UW2). This break in behaviour at UV wave-

lengths, and the huge difference in the outburst durations indicates that the X-ray origin is intrinsically distinct from the optical, and hence infers the presence of multiple emitting regions.

The brevity of the SSS phase ($\leq 15\text{d}$), together with the high temperatures ($\sim 90\text{--}110\text{eV}$) from both blackbody and WD atmosphere models, provides an indication that the white dwarf in MAXI J0158-744 is massive. According to Nomoto et al. (2007) such temperatures are only reached in white dwarfs exceeding $1.3 M_{\odot}$. Furthermore, the SSS light-curve of MAXI J0158-744 is very similar to that of the very fast classical nova V2491 Cyg, whose SSS phase was only 10d. This led Hachisu & Kato (2009) to infer a white dwarf mass of $\sim 1.3 M_{\odot}$.

3.2. Origin of the X-ray spectral features

Early in the outburst, the *Swift*/XRT spectra (Fig 2) required additional spectral features (a broad emission line at $\sim 0.7 \text{ keV}$ and an absorption edge at 0.89 keV). These could be associated with O, Fe and Ne features, where the broad 0.7 keV emission is a combination of OVIII Ly α (650 eV), Fe L ($700\text{--}720 \text{ eV}$), and Ne K (850 eV) lines; and the 0.89 keV absorption edge could be associated with the K-edge of OVIII (0.88 keV). A similar absorption edge has been observed in another SSS, RX J0925.7-4758, which is undergoing steady nuclear burning on the white dwarf surface (Ebisawa et al. 1996).

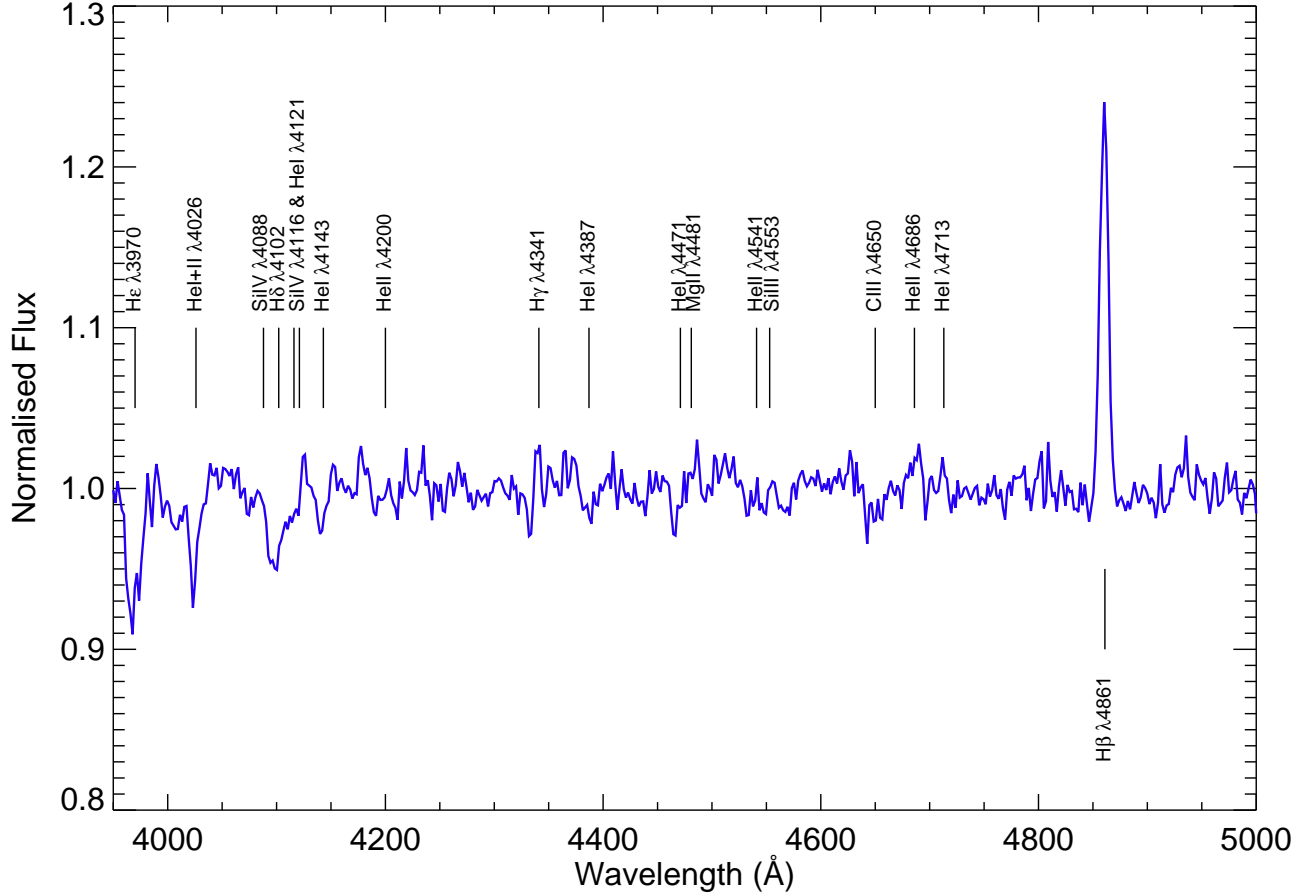


FIG. 5.— Blue spectrum of MAXI J0158-744 obtained with the NTT on 2011-12-08. The spectrum has been normalized to remove the continuum and redshift corrected by -158 km s^{-1} . Transitions relevant to spectral classification are marked.

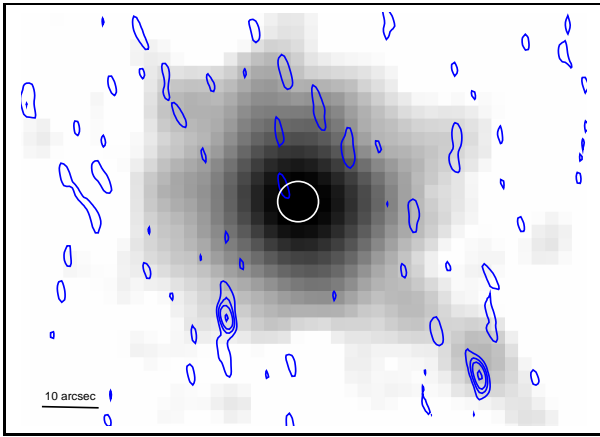


FIG. 6.— 1- σ , 2- σ , and 3- σ contours (blue) of the ATCA data are shown with a smoothed 25 ks *Swift*/XRT (0.2–2 keV) image. The white circle indicates the XRT position of MAXI J0158-744 with uncertainty $3.6''$ estimated by *xrtcentroid*. Within the error circle, no significant radio source was detected, but a very marginal signal ($< 2\sigma$) was seen at the edge of the circle.

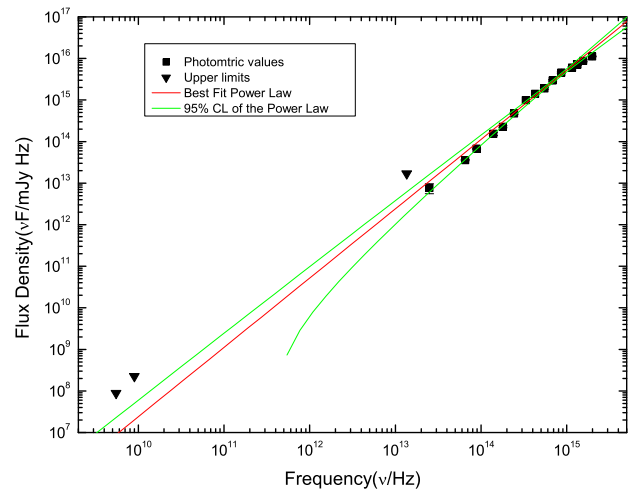


FIG. 7.— MAXI J0158-744 SED obtained by combining the ATCA radio data (upper limits at 5.5 GHz and 9 GHz); w1 ($3.4\mu\text{m}$), w2 ($4.6\mu\text{m}$), w3 ($12\mu\text{m}$), w4 ($22\mu\text{m}$) from the WISE catalog; I and R from SuperCOSMOS; UVW1, UVM2, UVW2, U, B, and V from *Swift* UVOT; and NUV, FUV from the GALEX. The SED can be described by a power law of index about 1.7.

Consequently, the K-edge and 0.7 keV broad emission features also support the interpretation of MAXI J0158-744 as an accreting white dwarf system. Their origin is likely to be in the ejected shell from the white dwarf sur-

face at the beginning of the strong outburst, following which the white dwarf enters a luminous supersoft phase (King & Pounds 2003). This provides further support for

MAXI J0158-744 containing a massive ($\geq 1.3M_{\odot}$) white dwarf.

3.3. Origin of the initial X-ray flash

So far we have concentrated on the analysis and interpretation of the *Swift*/XRT and UV/optical observations of MAXI J0158-744. However, perhaps the most remarkable feature of this outburst is the initial X-ray flash detected by the MAXI/GSC. Having established now that MAXI J0158-744 is in the SMC, then the luminosity of this flash, assuming a ~ 1 keV thermal (Raymond-Smith) plasma model, is $\sim 2 \times 10^{39} (d/61.3 \text{ kpc})^2 \text{ erg s}^{-1}$ (2–4 keV). During that single orbit, MAXI J0158-744 outshone the luminous neutron-star X-ray binary, SMC X-1, in the MAXI/GSC 2–4 keV energy band. Even more remarkably, the flash was very short-lived, rising and falling in < 92 mins by at least a factor 20, as MAXI detected no source at that location in the orbits before and after the X-ray flash.

The first *Swift* observation was approximately 10 hours later, and revealed the lower temperature SSS component, which we believe is quite distinct from the harder X-ray flash. That is because, even though the SSS flux declined over subsequent days, the timescale for this was much longer than the dramatic drop of the X-ray flash. Consequently, we should consider alternative emission mechanisms for the X-ray flash.

Firstly, we have now argued that many of the MAXI J0158-744 properties are accountable as a nova explosion, and these can lead to hard X-ray components being present, as well as a short-lived SSS phase (see e.g. Mukai et al. (2008) and references therein). An excellent example of this is the recurrent nova, RS Oph, that underwent a well-studied outburst in 2006 (Sokoloski et al. 2006), reaching a hard X-ray luminosity of $\sim 10^{36} \text{ erg s}^{-1}$ which included Fe K α emission. This was explained as the result of a $\sim 3500 \text{ km s}^{-1}$ ejected nova shell hitting the wind of the M giant donor star, essentially a “mini-SNR” as the subsequent X-ray decline followed a typical Sedov light-curve. However, in some cases, the X-ray properties imply that the emission originates internal to the nova ejecta, and so internal shock models have been developed (Mukai & Ishida 2001). Nevertheless, the X-ray luminosities attained are usually $\leq 10^{35} \text{ erg s}^{-1}$.

But much higher luminosities are possible in special circumstances. The 1998 X-ray transient, XTE J0421+560, was associated with the bright B[e] star, CI Cam, and initially interpreted as the periastron passage of a neutron star or black hole compact object through the dense equatorial outflow from the B[e] star (Hynes et al. 2002), producing a peak X-ray luminosity of $\sim 3 \times 10^{37} (d/2 \text{ kpc})^2 \text{ erg s}^{-1}$ (3–20 keV). However, CI Cam has properties that did not fit well with other HMXBs or soft X-ray transients, and this led Filippova et al. (2008) to propose that XTE J0421+560 was actually a nova explosion on an accreting white dwarf in its 19d, eccentric orbit. While this interpretation, and the nature of the compact object in CI Cam, remains controversial, the detailed analysis by Filippova et al. (2008) of a nova explosion in the surroundings of an early-type star remain directly applicable to MAXI J0158-744. The large increase in luminosity compared to RS Oph they explain as due to the much denser medium that surrounds

the B[e] star. The ejected nova shell interacts with and shocks the B[e] wind creating a hot ($\sim 1\text{--}10 \text{ keV}$) thermal plasma that both heats and cools rapidly. In the case of XTE J0421+650 there was sufficient coverage to follow the rise and fall of this flux by a factor of 10 in $< 1 \text{ d}$ (Filippova et al. 2008). This is possible given a dense B[e] wind ($\sim 10^{10} \text{ cm}^{-3}$), which the shock will increase by a factor 4, and will radiatively cool on the observed timescale.

We therefore consider whether the detailed calculations of Filippova et al. (2008) can be applied to MAXI J0158-744, and what the implied parameters of the system would be. They give the timescale for radiative cooling as $\sim 3kT/2\Lambda n$, where Λ is the emissivity of a hot gas, and is $\sim 10^{-24} \text{ erg cm}^3 \text{ s}^{-1}$ in the 2–20 keV band for $kT \sim 1 \text{ keV}$. The MAXI J0158-744 X-ray flash cooled in $\sim 4000 \text{ s}$, and this requires $n \sim 5 \times 10^{11} \text{ cm}^{-3}$. Allowing for the factor 4 increase by the shock, this is only a factor 10 higher than that inferred for CI Cam by Filippova et al. (2008), and entirely reasonable for the enhanced density in the equatorial outflow of a rapidly rotating Be star.

Unfortunately, we do not yet know the orbital period of the MAXI J0158-744 system, but we assume 10d in order to make it more compact, and hence a higher density circumbinary medium. Taking the B1/2IIIe donor as $\sim 10M_{\odot}$ and a massive ($1.3M_{\odot}$) white dwarf, then a 10d period gives an orbital separation, $a \sim 1.5 \times 10^{13} \text{ cm}$. We can then use the order of magnitude calculation of the resulting shocked X-ray luminosity, L_{CBM} , from Itoh & Hachisu (1990):

$$L_{\text{CBM}} = 3 \times 10^{33} \frac{\Lambda}{10^{-23} \text{ erg cm}^3 \text{ s}^{-1}} \frac{M_{\text{CBM}}^2}{10^{-6} M_{\odot}} \times \frac{r_{\text{CBM}}^{-2}}{10^{15} \text{ cm}} \frac{r_s^{-1}}{10^{15} \text{ cm}} \text{ erg s}^{-1}, \quad (1)$$

where CBM refers to “circumbinary medium”, and r_s is the radius of the shock wave. Taking both r_s and $r_{\text{CBM}} \sim a$, and $M_{\text{CBM}} \sim 10^{-6} M_{\odot}$ (at least this much is normally ejected in a nova explosion), then $L_{\text{CBM}} \sim 10^{39} \text{ erg s}^{-1}$. This is an order of magnitude or so above that of CI Cam, but the BeX in the SMC have well established, dense equatorial outflows as a result of their rapid rotation (Hynes et al. 2002; Madura et al. 2007) and so these parameters are by no means extreme. Furthermore, if the compact object is a massive O-Ne-Mg white dwarf, then enhanced X-ray emission features at the energies seen in our *Swift*/XRT spectra would be expected.

3.4. Be+WD systems in the Magellanic Clouds

There have already been two SSS discovered that appear to be associated with Be mass donors, the first, XMMU J052016.0-692505, in the LMC (Kahabka et al. 2006), the second, XMM J010147.5-715550, in the SMC (Sturm et al. 2012). The LMC SSS has $L_X > 10^{34} \text{ erg s}^{-1}$ whereas the SMC SSS is weaker, at $3 \times 10^{34} \text{ erg s}^{-1}$. Both are optically identified with Be systems, and appear to be persistent SSS. Consequently, they are both likely in the steady hydrogen burning phase, and neither have exhibited nova eruptions comparable to MAXI J0158-744. Interestingly, both have reported very long periodicities

in their OGLE light-curves (~ 510 or 1020 d, and 1264 d for the LMC and SMC sources respectively), although these are not well constrained due to the limited monitoring timescale. However, such long-term periodicities are now a well established feature in SMC BeX sources (Rajaelimanana et al. 2011), in many of which the much shorter orbital periods are already well known. Consequently, we dismiss the long periods in these new SSS as being orbital in nature. And in any case, the orbital periods will have to be very much shorter in order to sustain the mass accretion necessary for steady hydrogen burning, as calculated in the previous section.

3.5. Comparison with QSS/SSS in nearby galaxies

Over the last decade, many large extragalactic surveys have been undertaken by Chandra and XMM in order to search for SSS and possibly related systems (so-called quasi-soft sources, or QSS) in nearby galaxies of the Local Group (Di Stefano & Kong 2003, 2004a; Di Stefano et al. 2004b; Kong & Di Stefano 2005). Some of the candidates discovered in these surveys have also reached “ultraluminous” levels, as well as displaying transient behavior. One of the best examples is ULX-1 in M101 (Kong & Di Stefano 2005). Apart from the much higher implied luminosity, MAXI J0158-744 is quite similar to M101 ULX-1 in many aspects (i.e. temperature, variability). Interestingly, M101 ULX-1 also has a massive companion, a B supergiant counterpart (Kuntz et al. 2005), close to a star formation region. Consequently, it is worth considering whether these are all examples of the same phenomenon.

A popular, but controversial, interpretation of extragalactic QSS and SSS is that they are extreme versions of the stellar-mass black hole systems in our Galaxy, wherein the compact object is a much higher, “intermediate mass” black hole (IMBH, $\geq 50 M_{\odot}$) in a soft/high accretion state (Di Stefano et al. 2010). However, by considering the similarities between these candidate IMBHs and MAXI J0158-744, we propose that some of the IMBH candidates could instead be a MAXI J0158-744-like object, consisting of a white dwarf accreting from a high mass donor and undergoing what are essentially classical or recurrent nova outbursts in a high density environment. According to the work of Di Stefano & Kong (2004a), some QSS/SSS may have high mass companions, based on their association with their host galaxy’s spiral arms. Unfortunately, the main focus of this work was still on the IMBH scenario and the nature of the high mass companion was not considered in detail.

In fact, more than 40 QSS/SSS candidates have been discovered in M31 by *Chandra* (Di Stefano et al. 2004b). All of them have low black-body temperatures, and some of them exhibit a harder power-law component in their spectra. After comparing them with our QSS/SSS candidate MAXI J0158-744, we propose that this kind of

spectrum could be fully explained by our Be+WD binary model, where the low temperature blackbody is indeed an accreting white dwarf and the hard power-law component can be attributed to the shock interaction of the nova shell/ejection with the hot stellar wind (or Be equatorial, outflowing disc). Unfortunately, the even greater distances of this population of QSS/SSS makes it very difficult to distinguish between various combinations of spectral models. It is therefore essential to obtain much higher quality spectra of these extragalactic systems, so as to probe the true nature of these supposedly IMBH systems.

In conclusion, we believe that MAXI J0158-744, located in the SMC, is a very important example of this extreme (apparently ultra-luminous X-ray flash followed by SSS) behaviour that a nova explosion can lead to if it is in the appropriate environment. It has pointed us in a new direction for understanding the QSS/SSS in external galaxies that have been proposed as IMBH associated with massive companions. If confirmed, it reveals an entirely new sub-class of SSS, showing once again that white dwarfs are capable of mimicking black holes, and possibly even (some) ULXs.

One of us (PAC) would like to thank Mike Bode, Koji Mukai and Valerio Ribeiro for stimulating discussions on the nature and properties of nova outbursts. We also thank Nicola Masetti (Primary Investigator of the project “Revealing the nature of southern hard X-ray sources through optical spectroscopy”) for the SAAO optical spectrum presented here. This project is supported by the National Science Council of the Republic of China (Taiwan) through grants NSC100-2628-M-007-002-MY3 and NSC100-2923-M-007-001-MY3. This research has made use of the MAXI data provided by RIKEN, JAXA and the MAXI team. This work is based on observations obtained with *Swift*, a part of NASA’s medium Explorer program, with the hardware being developed by an international team from the United States, the United Kingdom and Italy, with additional scientific involvement by France, Japan, Germany, Denmark, Spain, and South Africa. The OGLE project has received funding from the European Research Council under the European Community’s Seventh Framework Programme (FP7/2007-2013) / ERC grant agreement no. 246678 to AU. We thank the ATCA team for an allocation of Director’s Discretionary Time for this project. The Australia Telescope is funded by the Commonwealth of Australia for operation as a National Facility managed by CSIRO. This publication also makes use of data products from the Wide-field Infrared Survey Explorer, which is a joint project of the University of California, Los Angeles, and the Jet Propulsion Laboratory/California Institute of Technology, funded by the National Aeronautics and Space Administration.

REFERENCES

- Arnaud, K. A. 1996, *Astronomical Data Analysis Software and Systems V*, 101, 17
- Bird, A. J., Coe, M. J., McBride, V. A., & Udalski, A. 2012, *MNRAS*, 423, 3663
- Bufano, F., Immler, S., Turatto, M., et al. 2009, *ApJ*, 700, 1456
- Burrows, D. N., Hill, J. E., Nousek, J. A., et al. 2005, *Space Sci. Rev.*, 120, 165
- Capalbi, M., Perri, M., Saijia, B., Tamburelli, F., & Angelini, L. 2005, *Swift XRT Data Reduction Guide*, Version 1.2
- Cardelli, J. A., Clayton, G. C., & Mathis, J. S. 1989, *ApJ*, 345, 245
- Clark, J. S., Miroshnichenko, A. S., Larionov, V. M., et al. 2000, *A&A*, 356, 50

- Crampton, D., Cowley, A. P., Hutchings, J. B., et al. 1987, *ApJ*, 321, 745
- Dickey, J. M., & Lockman, F. J. 1990, *ARA&A*, 28, 215
- Diplas, A., & Savage, B. D. 1993, *Massive Stars: Their Lives in the Interstellar Medium*, 35, 289
- Di Stefano, R., & Kong, A. K. H. 2003, *ApJ*, 592, 884
- Di Stefano, R., & Kong, A. K. H. 2004a, *ApJ*, 609, 710
- Di Stefano, R., Kong, A. K. H., Greiner, J., et al. 2004b, *ApJ*, 610, 247
- Di Stefano, R. 2010, *ApJ*, 712, 728
- Di Stefano, R., Primi, F. A., Liu, J., Kong, A., & Patel, B. 2010, *Astronomische Nachrichten*, 331, 205
- Ebisawa, K., Asai, K., Mukai, K., et al. 1996, *Supersoft X-Ray Sources*, 472, 91
- Filippova, E. V., Revnivtsev, M. G., & Lutovinov, A. A. 2008, *Astronomy Letters*, 34, 797
- Gordon, K. D., Clayton, G. C., Misselt, K. A., Landolt, A. U., & Wolff, M. J. 2003, *ApJ*, 594, 279
- Greiner, J. 2000, *New Astr.*, 5, 137
- Hachisu, I., & Kato, M. 2009, *ApJ*, 694, L103
- Hambly, N. C., MacGillivray, H. T., Read, M. A., et al. 2001, *MNRAS*, 326, 1279
- Hambly, N. C., Irwin, M. J., & MacGillivray, H. T. 2001, *MNRAS*, 326, 1295
- Hambly, N. C., Davenhall, A. C., Irwin, M. J., & MacGillivray, H. T. 2001, *MNRAS*, 326, 1315
- Hilditch, R. W., Howarth, I. D., & Harries, T. J. 2005, *MNRAS*, 357, 304
- Hodges-Kluck, E. J., Bregman, J. N., Miller, J. M., & Pellegrini, E. 2012, *ApJ*, 747, L39
- Hynes, R. I., Clark, J. S., Barsukova, E. A., et al. 2002, *A&A*, 392, 991
- Itoh, H., & Hachisu, I. 1990, *ApJ*, 358, 551
- Juett, A. M., Psaltis, D., & Chakrabarty, D. 2001, *ApJ*, 560, L59
- Kahabka, P., van den Heuvel, E.P.J. 2006, in *Compact stellar X-ray sources*
- Kahabka, P., Haberl, F., Payne, J. L., & Filipović, M. D. 2006, *A&A*, 458, 285
- Kato, M. 2010, *Astronomische Nachrichten*, 331, 140
- Kennea, J.A. et al. 2011, *Atel*, 3758
- Kimura, M. et al. 2011, *Atel*, 3756
- King, A. R., & Pounds, K. A. 2003, *MNRAS*, 345, 657
- Kong, A. K. H., Di Stefano, R., & Yuan, F. 2004, *ApJ*, 617, L49
- Kong, A. K. H., & Di Stefano, R. 2005, *ApJ*, 632, L107
- Kuntz, K. D., Gruendl, R. A., Chu, Y.-H., et al. 2005, *ApJ*, 620, L31
- Lennon, D. J. 1997, *A&A*, 317, 871
- Li, K.L., & Kong, A. K. H. 2011, *Atel*, 3765
- Li, K.L., Kong, A. K. H., Tam, P.H.T. & Wu, J.H.K. 2011, *Atel*, 3759
- Long, K. S., Helfand, D. J., & Grabelsky, D. A. 1981, *ApJ*, 248, 925
- Madej, O. K., Jonker, P. G., Fabian, A. C., et al. 2010, *MNRAS*, 407, L11
- Madej, O. K., & Jonker, P. G. 2011, *MNRAS*, 412, L11
- Madura, T. I., Owocki, S. P., & Feldmeier, A. 2007, *ApJ*, 660, 687
- Mioduszewski, A. J., & Rupen, M. P. 2004, *ApJ*, 615, 432
- Mukai, K., & Ishida, M. 2001, *ApJ*, 551, 1024
- Mukai, K., Orio, M., & Della Valle, M. 2008, *A Population Explosion: The Nature & Evolution of X-ray Binaries in Diverse Environments*, 1010, 143
- Nandra, K., Laird, E. S., Adelberger, K., et al. 2005, *MNRAS*, 356, 568
- Nishiyama, S., Haba, Y., Kato, D., et al. 2007, *ApJ*, 658, 358
- Nomoto, K., Nariai, K., & Sugimoto, D. 1979, *PASJ*, 31, 287
- Nomoto, K., Saio, H., Kato, M., & Hachisu, I. 2007, *ApJ*, 663, 1269
- Paczynski, B., & Zytow, A. N. 1978, *ApJ*, 222, 604
- Rajaelimanana, A. F., Charles, P. A., & Udalski, A. 2011, *MNRAS*, 413, 1600
- Rauch, T., & Deetjen, J. L. 2003, *Stellar Atmosphere Modeling*, 288, 103
- Roming, P. W. A., Kennedy, T. E., Mason, K. O., et al. 2005, *Space Sci. Rev.*, 120, 95
- Russell, S. C., & Dopita, M. A. 1992, *ApJ*, 384, 508
- Sokoloski, J. L., Luna, G. J. M., Mukai, K., & Kenyon, S. J. 2006, *Nature*, 442, 276
- Soria, R., Kuntz, K. D., Winkler, P. F., et al. 2012, *ApJ*, 750, 152
- Sault, R. J., Teuben, P. J., & Wright, M. C. H. 1995, *Astronomical Data Analysis Software and Systems IV*, 77, 433
- Sault, R. J., & Conway, J. E. 1999, *Synthesis Imaging in Radio Astronomy II*, 180, 419
- Shipman, H. L. 1979, *ApJ*, 228, 240
- Sienkiewicz, R. 1980, *A&A*, 85, 295
- Sion, E. M., Acierno, M. J., & Tomczyk, S. 1979, *ApJ*, 230, 832
- Skrutskie, M. F., Cutri, R. M., Stiening, R., et al. 2006, *AJ*, 131, 1163
- Smith, D. A., & Remillard, R. 2003, *The Astronomer's Telegram*, 129, 1
- Southwell, K. A., Livio, M., Charles, P. A., O'Donoghue, D., & Sutherland, W. J. 1996, *ApJ*, 470, 1065
- Sturm, R., Haberl, F., Pietsch, W., et al. 2012, *A&A*, 537, A76
- Swartz, D. A., Ghosh, K. K., Tennant, A. F., & Wu, K. 2004, *ApJS*, 154, 519
- Tozzi, P., Gilli, R., Mainieri, V., et al. 2006, *A&A*, 451, 457
- Trümper, J., Hasinger, G., Aschenbach, B., et al. 1991, *Nature*, 349, 579
- Udalski, A. 2008, *Acta Astron.*, 58, 187
- van den Heuvel, E. P. J., Bhattacharya, D., Nomoto, K., & Rappaport, S. A. 1992, *A&A*, 262, 97
- Walborn, N. R., & Fitzpatrick, E. L. 1990, *PASP*, 102, 379
- Werner, K., & Dreizler, S. 1999, *Journal of Computational and Applied Mathematics*, 109, 65
- Werner, K., Deetjen, J. L., Dreizler, S., et al. 2003, *Stellar Atmosphere Modeling*, 288, 31
- Yan, J., Liu, Q., & Hang, H. 2007, *AJ*, 133, 1478
- Zampieri, L., & Roberts, T. P. 2009, *MNRAS*, 400, 677